DOI: 10.14258/jcprm.20260419194

UDC 547.992.3:544.18

# EFFECT OF SULFATION ON STRUCTURAL, ELECTRONIC AND VIBRATIONAL PROPERTIES OF 4-O-5 LIGNIN DIMER: A DFT STUDY

© ***A.S. Kazachenko[1,2,3*], F. Akman[4], U. Holikulov[5], A. Jumabaev[5], Yu.N. Malyar[2,3]***

*[1] Reshetnev Siberian State University of Science and Technology, ave. Mira, 82, Krasnoyarsk, 660037, Russia, leo_lion_leo@mail.ru*
*[2] Siberian Federal University, ave. Svobodny, 79, Krasnoyarsk, 660041, Russia*
*[3] Institute of Chemistry and Chemical Technology, Krasnoyarsk Science Center, Siberian Branch, Russian Academy of Sciences, Akademgorodok, 50/24, Krasnoyarsk, 660036, Russia*
*[4] University of Bingöl, Bingöl, 12000, Turkey*
*[5] Samarkand State University, University Blvd., 15, Samarkand, 140104, Uzbekistan*

In the present work, a comparative study of the geometric, electronic and vibrational characteristics of the initial 4-O-5 lignin dimer and its sulfated form was performed using the density functional theory (DFT) method at the B3LYP/6-31G(d,p) level. The optimized molecular structures showed that the introduction of the sulfate group leads to significant changes in the C5-O7 and O7-C8 bond lengths, as well as in the bond angles associated with the ether bridge, indicating a redistribution of the electron density. Mulliken and APT charge analyses revealed an increased negative density on the oxygen atoms of the sulfate group and a positive charge on sulfur, indicating its strong electron-withdrawing character. An increase in the HOMO–LUMO energy gap from 5.408 eV to 5.570 eV after sulfation indicates an increase in the kinetic stability of the molecule. However, the growth in electronegativity (χ) and electrophilicity index (ω) indicate an increased tendency to electrophilic reactions. Molecular electrostatic potential (MEP) surfaces confirmed the increase in negative potential in the region of the sulfate group, which explains the improved hydrophilicity and solubility. Theoretical IR spectra show characteristic S-O bands at 1310, 1102, 861 and 655 $cm^{-1}$, confirming the successful modeling of the sulfate derivative. The data obtained contribute to the understanding of the mechanisms of lignin modification and its behavior in biorefining processes and the synthesis of bioactive compounds.

*Keywords*: lignin, sulfated lignin, DFT, lignin model compounds.

**For citing:** Kazachenko A.S., Akman F., Holikulov U., Jumabaev A., Malyar Yu.N. *Khimiya Rastitel'nogo Syr'ya*, 2026, no. 4, Online First. (in Russ.). https://doi.org/10.14258/jcprm.20260419194.

***Introduction***

Lignin is one of the most common biopolymers on Earth, second only to cellulose in mass fraction. It is a complex three-dimensional polyphenolic polymer formed mainly from derivatives of coniferyl, sinapyl and p-coumaryl alcohols linked by various C-O and C-C bonds [1]. Due to its aromatic nature and high content of functional groups, lignin is considered a promising renewable source for the production of biopolymers, fuels, platform chemicals and functional materials [2, 3]. However, its high hydrophobicity, tendency to aggregation and complex structure limit its use in industrial processes [4].

One of the effective methods for modifying lignin is sulfation – the introduction of sulfate ($-OSO_3^-$) or sulfone ($-SO_3^-$) groups, which significantly increases its hydrophilicity, and accordingly solubility in water and reactivity [5–7]. Such modified forms of lignin are used as dispersants, surfactants, components of polymer composites and carriers in pharmaceuticals [8]. In particular, lignin with anionic functional groups demonstrates improved compatibility with polar matrices and increased stability in aqueous solutions [9]. Due to the three-dimensional irregular structure of lignin, it is very difficult to carry out controlled modification of the polymer and predict the chemical and biological properties of its sulfated derivatives.

* Corresponding author.

Quantum-chemical methods are widely used to understand the effect of sulfation on the molecular properties of lignin, especially density functional theory (DFT), which allows for highly accurate modeling of the geometry, electronic structure and spectroscopic characteristics of model compounds [10]. Dimers that imitate the main structural fragments of lignin, such as β-O-4, 5-5, β-5 and 4-O-5 bonds, are often used as model systems [11–13]. The 4-O-5 bond, though less abundant than β-O-4 (typically 3–8% in woody lignins and almost absent in herbaceous plants [14]), is one of the most resistant linkages due to its diphenyl ether structure. Despite its low content, the high stability of the 4-O-5 bond makes it a critical target for understanding the limits of chemical and enzymatic lignin degradation. Therefore, studying the sulfation of this particular fragment provides valuable insights into how modification affects the most recalcitrant parts of the lignin polymer, complementing studies on more common linkages such as β-O-4.

Modification of this fragment can significantly affect its stability and reactivity. In this work, a systematic DFT study of the effect of sulfation on the 4-O-5 lignin dimer is presented for the first time. Geometric optimization, electron density analysis, calculation of frontier molecular orbitals (HOMO and LUMO), molecular electrostatic potential (MEP) and theoretical IR spectra were performed at the B3LYP/6-31G(d,p) level. The data obtained allow a deeper understanding of how chemical modification affects the electronic and steric properties of lignin, which is of key importance for the development of effective strategies for its processing and functionalization within the framework of the biorefining concept [15].

***Computational details***

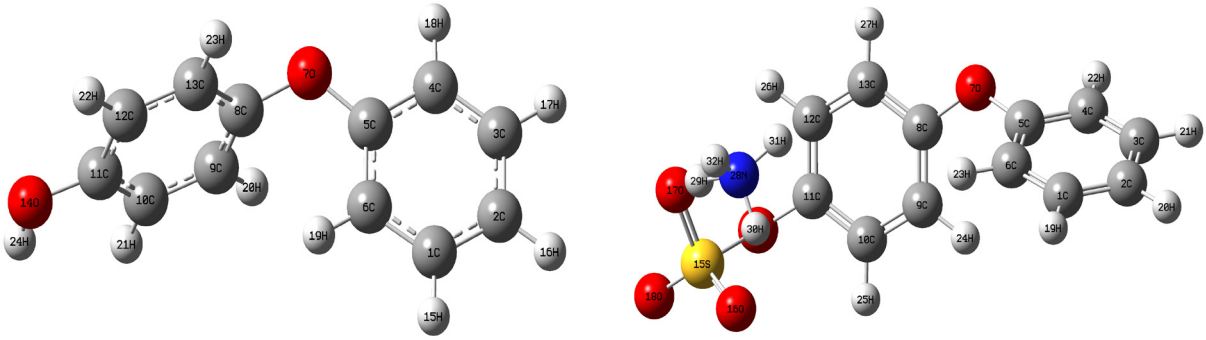
The 4-O-5 structure with one reactive hydroxyl group (4-phenoxyphenol) was used as a model lignin dimer. Sulfation of this molecule occurs by the formation of an ester bond, with the introduction of an anionic sulfate group $–OSO_3^-$ stabilized by an ammonium cation ($NH_4^+$) into the structure. For a comprehensive investigation of the electronic and structural characteristics of the 4-O-5 lignin dimer and its sulfated derivative, density functional theory (DFT) calculations were carried out using the B3LYP functional in conjunction with the 6-31G(d,p) basis set [16, 17]. All computations were performed in the gas phase employing the Gaussian 09W software package [18], while molecular structures were visualized using GaussView 6.0 [19]. The equilibrium geometries were fully optimized to locate the global energy minima, and their stability was verified by means of harmonic vibrational frequency analysis, confirming the absence of imaginary frequencies. To predict the infrared (IR) spectra and evaluate the impact of sulfation on vibrational modes, harmonic frequencies were calculated and scaled by a factor of 0.9608 to correct for systematic deviations from experimental values. The frontier molecular orbitals (HOMO and LUMO) were analyzed to determine the energy gap and assess the chemical reactivity and kinetic stability of the compounds. Global reactivity descriptors, derived from conceptual DFT, were computed to further characterize the reactivity trends. Additionally, molecular electrostatic potential (MEP) surfaces were mapped to identify regions of high electron density (nucleophilic sites) and electron deficiency (electrophilic sites), providing insights into the intermolecular interaction preferences and reactive centers of the studied systems.

***Results and discussions***

It should be noted that all calculations were carried out in the gas phase without explicit solvation or counterion effects beyond the ammonium cation used to neutralize the sulfate group. While this approach allows a clear assessment of the intrinsic electronic and steric effects of sulfation, it does not fully capture the influence of aqueous environments or polar solvents. Future studies could incorporate implicit solvation models (e.g., PCM, SMD) to better represent realistic conditions. Nevertheless, the gas-phase DFT results provide a solid baseline for understanding the molecular-level changes induced by sulfation.

Optimization of the geometry of the studied structures is the first important step in their detailed theoretical study [20, 21]. Figure 1 shows the optimized molecular structures of two forms of lignin obtained by quantum-chemical calculation at the B3LYP/6-31G(d,p) level of theory: a) classical 4-O-5 lignin dimer and b) its sulfated derivative – 4-O-5 lignin sulfate.

Figure 1 visualizes the geometric configurations of the molecules in their energetically lowest (ground) states, which allows for a detailed analysis of the spatial organization of aromatic rings, ether bridges (C-O-C) and introduced sulfate groups. Comparison of the structures shows the effect of sulfation on the electron distribution, conformational flexibility and steric parameters of the molecule. The introduction of a sulfate group at the 4-O-5 position results in significant changes in interatomic distances, bond angles, and likely an increase in the polarity and solubility of the compound, which has important implications for understanding the reactivity of lignin in chemical and biochemical processing.




*a* *b*

Fig. 1. Optimized molecular structure of *a*) 4-O-5 lignin dimer and *b*) 4-O-5 sulfated lignin dimer, calculated at the B3LYP/6-31G(d,p) level of theory

The use of the B3LYP hybrid functional in combination with the 6-31G(d,p) polarization basis set provides a highly accurate description of the electronic structure and geometry of organic molecules, including systems with delocalized π-electrons, such as lignin [22]. This level of theory is widely used to model the structural and electronic properties of polymer-like dimers and has proven itself in predicting thermodynamic parameters and reactivity [23, 24]. The data obtained are consistent with previously published studies showing that lignin modification by sulfation increases its hydrophilicity and reduces its tendency to aggregation, which is important for use in the production of biosynthetic polymers, sulfonated surfactants, and drug delivery systems [25]. In addition, quantum chemical modeling of such systems allows predicting lignin degradation pathways under the action of catalytic and enzymatic systems, which is important for biorefinery processes – i.e., the integrated fractionation and conversion of lignocellulosic biomass into value-added products, including biofuels, platform chemicals, and functional materials. Theoretical modeling of sulfated lignin dimers helps to predict their degradation pathways under catalytic or enzymatic conditions, thereby guiding experimental efforts in lignin valorization [26].

Table 1 presents the results of geometric optimization of 4-O-5 lignin (a) and its sulfate derivative (b) molecules in the ground state. The lengths of covalent bonds and valence angles characterizing the equilibrium conformation of the molecules are given. For 4-O-5 lignin, the lengths of aromatic bonds C1-C2, C1-C6, C2-C3, C3-C4, C4-C5, C5-C6 are in the range from 1.3923 Å (C12-C13) to 1.3988 Å (C4-C5), which is typical for delocalized aromatic systems. The lengths of C-H bonds vary from 1.0838 Å (C6-H19) to 1.0879 Å (C10-H21). The key bonds that determine the ether bridge bond are C5-O7 (1.3797 Å) and O7-C8 (1.3878 Å). The angles in the aromatic rings are close to 120°, for example, C2-C1-C6 is 120.9056°, confirming the sp2 hybridization of carbon.

Comparison of the parameters allows us to estimate the influence of the sulfate group on the molecular geometry. In the 4-O-5 lignin sulfate (b) molecule, the lengths of the aromatic bonds are also within the range of 1.3932 Å (C12-C13) – 1.4001 Å (C8-C13). However, some change in the bond lengths is observed in key areas. The C5-O7 bond length increases from 1.3797 Å to 1.3864 Å, and the O7-C8 bond length decreases to 1.3770 Å compared to the starting compound (a). This may indicate a change in the nature of delocalization of the electron density in this fragment. The new bonds associated with the sulfate group have the following lengths: O14-S15 (1.6635 Å), S15-O16 (1.4639 Å), S15-O17 (1.5769 Å), and S15-O18 (1.4440 Å). The O17-H29 bond (1.0586 Å) is also present, indicating the possible presence of a hydroxyl group in the sulfate fragment. The bond angles also undergo changes; for example, the angle C4-C5-O7 increases from 115.7452° to 117.3223°, and the angle C5-O7-C8 increases from 119.9905° to 120.9716°. The angles characterizing the geometry around the sulfur atom S15, such as O14-S15-O16 (107.7897°), O14-S15-O17 (102.2379°), O14-S15-O18 (103.8623°), O16-S15-O17 (109.084°), O16-S15-O18 (121.7709°), O17-S15-O18 (110.1863°), are also consistent with the expected tetrahedral (or distorted tetrahedral) geometry for sulfate compounds. These changes reflect the influence of the inductive and mesomeric effects of the sulfate group on the electron density and, accordingly, on the structure of the molecular [10, 21]. The C-O and C-C lengths in the aromatic fragments are consistent with the literature data for similar compounds [25].

Table 2 shows the electron density distribution in 4-O-5 lignin (a) and 4-O-5 lignin sulfate (b) molecules calculated by two different methods: Mulliken Population Analysis (MPA) and Atomic Polar Tensors (APT).

Table 1. Optimized bond parameters of a) 4-O-5 lignin dimer and b) 4-O-5 sulfated lignin dimer , calculated at the B3LYP/6-31G(d,p) level of theory

| a | | b | |
|---|---|---|---|
| *1* | | *2* | |
| Bond Lengths (Å) | | | |
| C1-C2 | 1.3946 | C1-C2 | 1.3966 |
| C1-C6 | 1.3966 | C1-C6 | 1.3947 |
| C1-H15 | 1.0864 | C1-H19 | 1.086 |
| C2-C3 | 1.3975 | C2-C3 | 1.3959 |
| C2-H16 | 1.0854 | C2-H20 | 1.0854 |
| C3-C4 | 1.3924 | C3-C4 | 1.3953 |
| C3-H17 | 1.0862 | C3-H21 | 1.0858 |
| C4-C5 | 1.3988 | C4-C5 | 1.3944 |
| C4-H18 | 1.085 | C4-H22 | 1.0847 |
| C5-C6 | 1.3976 | C5-C6 | 1.3972 |
| C5-O7 | 1.3797 | C5-O7 | 1.3864 |
| C6-H19 | 1.0838 | C6-H23 | 1.0849 |
| O7-C8 | 1.3878 | O7-C8 | 1.377 |
| C8-C9 | 1.3949 | C8-C9 | 1.3994 |
| C8-C13 | 1.3954 | C8-C13 | 1.4001 |
| C9-C10 | 1.3943 | C9-C10 | 1.3943 |
| C9-H20 | 1.0849 | C9-H24 | 1.0836 |
| C10-C11 | 1.3994 | C10-C11 | 1.3933 |
| C10-H21 | 1.0879 | C10-H25 | 1.0839 |
| C11-C12 | 1.3989 | C11-C12 | 1.3955 |
| C11-O14 | 1.3678 | C11-O14 | 1.3976 |
| C12-C13 | 1.3923 | C12-C13 | 1.3932 |
| C12-H22 | 1.0846 | C12-H26 | 1.0842 |
| C13-H23 | 1.0849 | C13-H27 | 1.0848 |
| O14-H24 | 0.966 | O14-S15 | 1.6635 |
| | | S15-O16 | 1.4639 |
| | | S15-O17 | 1.5769 |
| | | S15-O18 | 1.444 |
| | | O17-H29 | 1.0586 |
| | | N28-H29 | 1.5366 |
| | | N28-H30 | 1.0189 |
| | | N28-H31 | 1.0172 |
| | | N28-H32 | 1.0164 |
| Bond Angles (º) | | | |
| C2-C1-C6 | 120.9056 | C2-C1-C6 | 120.4811 |
| C2-C1-H15 | 120.035 | C2-C1-H19 | 120.0855 |
| C6-C1-H15 | 119.0589 | C6-C1-H19 | 119.4315 |
| C1-C2-C3 | 119.2959 | C1-C2-C3 | 119.6827 |
| C1-C2-H16 | 120.3478 | C1-C2-H20 | 120.1219 |
| C3-C2-H16 | 120.3563 | C3-C2-H20 | 120.1952 |
| C2-C3-C4 | 120.5258 | C2-C3-C4 | 120.381 |
| C2-C3-H17 | 120.1228 | C2-C3-H21 | 120.1375 |
| C4-C3-H17 | 119.3512 | C4-C3-H21 | 119.481 |
| C3-C4-C5 | 119.6548 | C3-C4-C5 | 119.3879 |
| C3-C4-H18 | 121.6127 | C3-C4-H22 | 121.6103 |
| C5-C4-H18 | 118.7325 | C5-C4-H22 | 119.0008 |
| C4-C5-C6 | 120.441 | C4-C5-C6 | 120.8346 |
| C4-C5-O7 | 115.7452 | C4-C5-O7 | 117.3223 |
| C6-C5-O7 | 123.7856 | C6-C5-O7 | 121.6889 |
| C1-C6-C5 | 119.1762 | C1-C6-C5 | 119.2293 |
| C1-C6-H19 | 120.5914 | C1-C6-H23 | 120.8903 |
| C5-C6-H19 | 120.2321 | C5-C6-H23 | 119.8803 |
| C5-O7-C8 | 119.9905 | C5-O7-C8 | 120.9716 |
| O7-C8-C9 | 121.0296 | O7-C8-C9 | 123.776 |
| O7-C8-C13 | 118.59 | O7-C8-C13 | 115.7769 |
| C9-C8-C13 | 120.2271 | C9-C8-C13 | 120.3712 |
| C8-C9-C10 | 119.7661 | C8-C9-C10 | 119.5427 |

*End of Table 1*

| *1* | | *2* | |
|---|---|---|---|
| C8-C9-H20 | 119.6957 | C8-C9-H24 | 120.2722 |
| C10-C9-H20 | 120.5378 | C10-C9-H24 | 120.1839 |
| C9-C10-C11 | 120.1558 | C9-C10-C11 | 119.8691 |
| C9-C10-H21 | 119.7905 | C9-C10-H25 | 120.8673 |
| C11-C10-H21 | 120.0512 | C11-C10-H25 | 119.2632 |
| C10-C11-C12 | 119.8273 | C10-C11-C12 | 120.817 |
| C10-C11-O14 | 122.7612 | C10-C11-O14 | 119.6947 |
| C12-C11-O14 | 117.4115 | C12-C11-O14 | 119.4266 |
| C11-C12-C13 | 119.9297 | C11-C12-C13 | 119.4729 |
| C11-C12-H22 | 118.9492 | C11-C12-H26 | 119.3558 |
| C13-C12-H22 | 121.121 | C13-C12-H26 | 121.1713 |
| C8-C13-C12 | 120.0912 | C8-C13-C12 | 119.922 |
| C8-C13-H23 | 119.0559 | C8-C13-H27 | 118.8325 |
| C12-C13-H23 | 120.851 | C12-C13-H27 | 121.2309 |
| C11-O14-H24 | 109.1499 | C11-O14-S15 | 117.0042 |
| | | O14-S15-O16 | 107.7897 |
| | | O14-S15-O17 | 102.2379 |
| | | O14-S15-O18 | 103.8623 |
| | | O16-S15-O17 | 109.084 |
| | | O16-S15-O18 | 121.7709 |
| | | O17-S15-O18 | 110.1863 |
| | | S15-O17-H29 | 109.8083 |
| | | H29-N28-H30 | 101.1678 |
| | | H29-N28-H31 | 111.952 |
| | | H29-N28-H32 | 117.7374 |
| | | H30-N28-H31 | 107.9865 |
| | | H30-N28-H32 | 108.7724 |
| | | H31-N28-H32 | 108.6048 |

For 4-O-5 lignin (a), the carbon atoms have Mulliken charges ranging from -0.14201 (C10) to 0.33275 (C11). The oxygen atoms O7 and O14 are strongly negatively charged: -0.57846 and -0.56008 (Mulliken), respectively. The hydrogen atoms bonded to oxygen (H24) have a positive charge of 0.31753. The Mulliken and APT charge values may differ, especially for the hydrogen and carbon atoms, due to the differences in the determination methods. For example, for the C1 atom the Mulliken charge is -0.09591, and the APT is 0.08269. The differences can be significant, as for the C2 atom: -0.08756 (Mulliken) and -0.12694 (APT).

In the sulfate molecule (b), a significant change in charge distribution is observed. The sulfur atom (S15) has a high positive charge: 1.3287 (Mulliken) and 2.44731 (APT), indicating its electron-withdrawing properties and high oxidation state (presumably +6). Accordingly, the oxygen atoms bound to sulfur (O16, O17, O18) carry a negative charge: O16 (-0.56306 Mulliken, -0.79438 APT), O17 (-0.60104 Mulliken, -1.00392 APT), O18 (-0.46303 Mulliken, -0.81092 APT). The oxygen atom O14, now bound to sulfur, also has a changed charge: -0.58154 (Mulliken) and -1.00316 (APT). The nitrogen atom N28 has a charge of -0.77225 (Mulliken) and -0.50974 (APT), and the hydrogen atoms bound to it H29-H32 have positive charges (H29: 0.43174 Mulliken, 0.62429 APT). The total charge of the molecule is close to zero, which confirms the correctness of the calculation. This charge distribution is important for understanding the reactivity of compounds, especially in the context of acid-base and redox processes, as well as intermolecular interactions such as hydrogen bonds [27].

Figure 2 is a visualization of the frontier molecular orbitals – highest occupied (HOMO) and lowest unoccupied (LUMO) – and the corresponding energy gaps (ΔE) calculated at the same quantum chemical level: B3LYP/6-31G(d,p). For the original 4-O-5 lignin dimer (Fig. 2a), the energy gap is ΔE = 5.408 eV, while for the sulfated form (Fig. 2b) it increases to ΔE = 5.561 eV. This indicates an increase in the kinetic stability of the molecule after sulfation, since a wider HOMO–LUMO gap is usually associated with lower chemical reactivity and greater stability towards external reagents [28, 29].

Analysis of the electron density distribution on HOMO and LUMO shows that in the initial form of lignin, electron delocalization is predominantly localized on the aromatic rings and the ether bridge, which is typical for π-conjugated systems. After sulfation, a density redistribution is observed with the participation of oxygen atoms of the sulfate group, which indicates the participation of this functional group in the electronic stabilization of the molecule. Such changes are of key importance for understanding the mechanisms of electrophilic substitution, radical degradation and catalytic modification of lignin in the processes of its bioprocessing and chemical utilization [30].

Table 2. Mulliken and APT charges of a) 4-O-5 lignin dimer and b) 4-O-5 sulfated lignin dimer, calculated at the B3LYP/6-31G(d,p) level of theory

| a | | | b | | |
|---|---|---|---|---|---|
| Atoms | Mulliken Charges | APT Charges | Atoms | Mulliken Charges | APT Charges |
| 1C | -0.09591 | 0.08269 | 1C | -0.09358 | 0.05076 |
| 2C | -0.08756 | -0.12694 | 2C | -0.08168 | -0.07973 |
| 3C | -0.09135 | 0.06659 | 3C | -0.09414 | 0.03275 |
| 4C | -0.11409 | -0.15696 | 4C | -0.10632 | -0.12504 |
| 5C | 0.32103 | 0.69463 | 5C | 0.30714 | 0.64535 |
| 6C | -0.11824 | -0.17603 | 6C | -0.09489 | -0.13802 |
| 7O | -0.57846 | -1.02561 | 7O | -0.573 | -1.09624 |
| 8C | 0.29853 | 0.49269 | 8C | 0.32964 | 0.7301 |
| 9C | -0.09722 | -0.03477 | 9C | -0.13224 | -0.15769 |
| 10C | -0.14201 | -0.09974 | 10C | -0.08297 | 0.02369 |
| 11C | 0.33275 | 0.56857 | 11C | 0.27155 | 0.38783 |
| 12C | -0.11247 | -0.1063 | 12C | -0.1012 | -0.0161 |
| 13C | -0.10874 | -0.00156 | 13C | -0.14536 | -0.15774 |
| 14O | -0.56008 | -0.74964 | 14O | -0.58154 | -1.00316 |
| 15H | 0.08657 | 0.01214 | 15S | 1.3287 | 2.44731 |
| 16H | 0.08134 | 0.01428 | 16O | -0.56306 | -0.79438 |
| 17H | 0.08661 | 0.01118 | 17O | -0.60104 | -1.00392 |
| 18H | 0.09463 | 0.04572 | 18O | -0.46303 | -0.81092 |
| 19H | 0.09981 | 0.05052 | 19H | 0.09382 | 0.01752 |
| 20H | 0.10331 | 0.04905 | 20H | 0.0915 | 0.02143 |
| 21H | 0.08054 | 0.00786 | 21H | 0.0963 | 0.01838 |
| 22H | 0.10181 | 0.0406 | 22H | 0.10337 | 0.05396 |
| 23H | 0.10167 | 0.051 | 23H | 0.08865 | 0.03616 |
| 24H | 0.31753 | 0.29003 | 24H | 0.11453 | 0.05622 |
| | | | 25H | 0.12087 | 0.05954 |
| | | | 26H | 0.1194 | 0.06236 |
| | | | 27H | 0.10667 | 0.05226 |
| | | | 28N | -0.77225 | -0.50974 |
| | | | 29H | 0.43174 | 0.62429 |
| | | | 30H | 0.31019 | 0.21711 |
| | | | 31H | 0.28804 | 0.17633 |
| | | | 32H | 0.28417 | 0.17931 |

Table 3 contains the fundamental descriptors of the density functional theory (DFT) that describe the global reactivities of molecules [31]. For 4-O-5 lignin (a), the HOMO energy is -5.7435 eV and LUMO is -0.3352 eV. The energy gap ($Eg = E_{LUMO} - E_{HOMO}$) is 5.4083 eV. The chemical hardness ($\eta = Eg/2$) is 2.7041 eV, and the chemical softness ($\zeta = 1/\eta$) is 0.3698 $eV^{-1}$. The electronegativity ($\chi = -(E_{HOMO} + E_{LUMO})/2$) is 3.0394 eV. The chemical potential ($\mu = -\chi$) is -3.0394 eV. The ionization potential ($IP \approx -E_{HOMO}$) is 5.7435 eV, and the electron affinity ($EA \approx -E_{LUMO}$) is 0.3352 eV. The electrophilicity index ($\omega = \chi^2/2\eta$) is 1.7081 eV. The nucleophilicity index ($N = E_{HOMO}$(molecule) - $E_{HOMO}$(reference nucleophile, e.g. water)) is 0.5854 (the value depends on the reference, the relative value is given here). The maximum charge transfer index ($\Delta Nmax = -\chi/\eta$) is 1.1240.

For 4-O-5 lignin sulfate (b), the descriptor values are different: $E_{HOMO}$ = -6.2624 eV, $E_{LUMO}$ = -0.6920 eV, Eg = 5.5704 eV, $\eta$ = 2.7852 eV, $\zeta$ = 0.3590 $eV^{-1}$, $\chi$ = 3.4772 eV, $\mu$ = -3.4772 eV, IP = 6.2624 eV, EA = 0.6920 eV, $\omega$ = 2.1706 eV, N = 0.4607, $\Delta Nmax$ = 1.2484. More negative $E_{HOMO}$ and $E_{LUMO}$ values for sulfate indicate lower energy levels of both occupied and unoccupied orbitals, which is associated with the electron-withdrawing influence of the sulfate group. Despite the wider energy gap (Eg=5.5704 eV compared to 5.4083 eV), the electronegativity ($\chi$=3.4772 eV) and electrophilicity index ($\omega$=2.1706 eV) are higher for the sulfate, indicating its higher tendency towards electrophilic reactions compared to the parent 4-O-5 lignin. The nucleophilicity index (N=0.4607) is lower than that of the parent compound (0.5854), consistent with a reduced tendency towards nucleophilic reactions. The chemical softness ($\zeta$=0.3590 $eV^{-1}$) is also slightly lower than that of 4-O-5 lignin (0.3698 $eV^{-1}$), consistent with the increased hardness ($\eta$=2.7852 eV compared to 2.7041 eV). The values of these parameters for 4-O-5 lignin sulfate indicate a change in its reactivity compared to the original lignin, which may be due to the presence of an electron-withdrawing sulfate group.

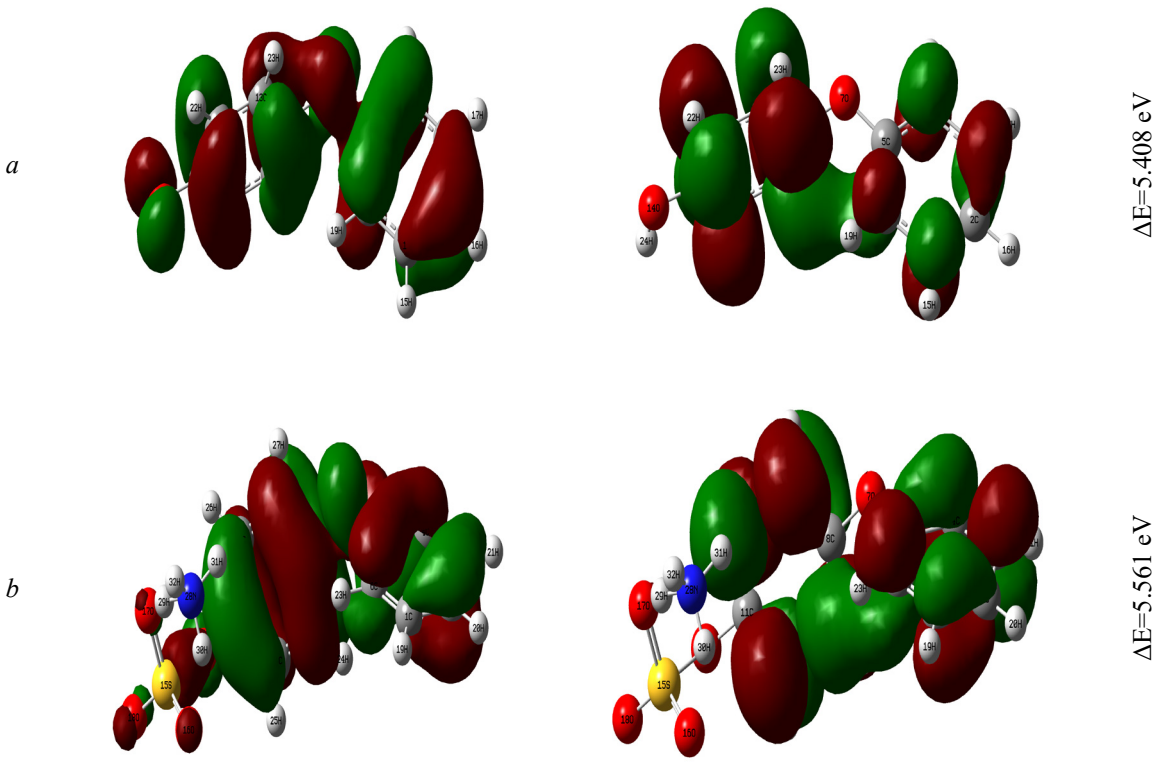



Fig. 2. HOMO, LUMO, and energy gaps of *a*) 4-O-5 lignin dimer and *b*) 4-O-5 sulfated lignin dimer, calculated at the B3LYP/6-31G(d,p) level of theory

Table 3. Energies of HOMO and LUMO, energy gap, chemical hardness, chemical softness, electronegativity, chemical potential, ionization potential, electron affinity, electrophilicity index, optical softness, nucleophilicity index, maximum charge transfer index of a) 4-O-5 lignin dimer and b) 4-O-5 sulfated lignin dimer, calculated at the B3LYP/6-31G(d,p) level of theory

| | **a** | **b** |
|---|---|---|
| $E_{HOMO}$ | -5.7435 | -6.2624 |
| $E_{LUMO}$ | -0.3352 | -0.6920 |
| Eg | 5.4083 | 5.5704 |
| η | 2.7041 | 2.7852 |
| ζ | 0.3698 | 0.3590 |
| χ | 3.0394 | 3.4772 |
| μ | -3.0394 | -3.4772 |
| IP | 5.7435 | 6.2624 |
| EA | 0.3352 | 0.6920 |
| ω | 1.7081 | 2.1706 |
| $\sigma_{\circ}$ | 0.1849 | 0.1795 |
| N | 0.5854 | 0.4607 |
| ΔNmax | 1.1240 | 1.2484 |

MEP analysis is a powerful tool for predicting reaction centers, intermolecular interactions and adsorption mechanisms, which makes it indispensable in the design of new lignin-containing materials [32]. Figure 3 illustrates the molecular electrostatic potential (MEP) surfaces and electrostatic potential distributions (ESP) for the 4-O-5 lignin dimer (a) and its sulfated form (b), calculated at the B3LYP/6-31G(d,p) level. The color scale reflects the charge density distribution: blue areas correspond to electron-deficient (electrophilic) sites, red ones to electron-excessive (nucleophilic) centers. In the original dimer, the highest negative density is localized on the oxygen atoms of the phenolic and ether groups, which makes them potential sites for electrophilic attacks. After sulfation, a significant increase in the negative potential in the region of the sulfate group is observed, which emphasizes its role as a strong nucleophile and a center of intermolecular polar interactions, including hydrogen bonds and ion-dipole interactions. This explains the improved hydration and solubility of modified lignin in aqueous media [33].

Table 4 compares the theoretically calculated (with a scaling factor of 0.9608 to improve agreement with experiment [25]) and experimentally determined infrared (IR) active vibrational frequencies for the two molecules. For 4-O-5 lignin (Fig.4a), the calculated frequencies include O-H (~3675 $cm^{-1}$), C-H (3095–3044 $cm^{-1}$), C=C (1607–1268 $cm^{-1}$), and C-O (1262, 1224, 1179 $cm^{-1}$) stretching vibrations. For 4-O-5 lignin sulfate (b), the calculated frequencies include N-H stretching vibrations (~3476–3337 $cm^{-1}$, as well as 2158, 1620, 1603, 1478 $cm^{-1}$, possibly related to deformation or combination vibrations), C-H (3105–3060 $cm^{-1}$), C=C (1597–1277 $cm^{-1}$), and C-O (1240, 1183, 1169 $cm^{-1}$). The characteristic frequencies of the S-O sulfate group are observed at 1310, 1102, 861, and 655 $cm^{-1}$. The presence of these frequencies in the theoretical spectrum confirms the successful modeling of the sulfate fragment. A wide range of N-H frequencies is also present, which may indicate the presence of hydrogen bonds or multiple N-H modes.

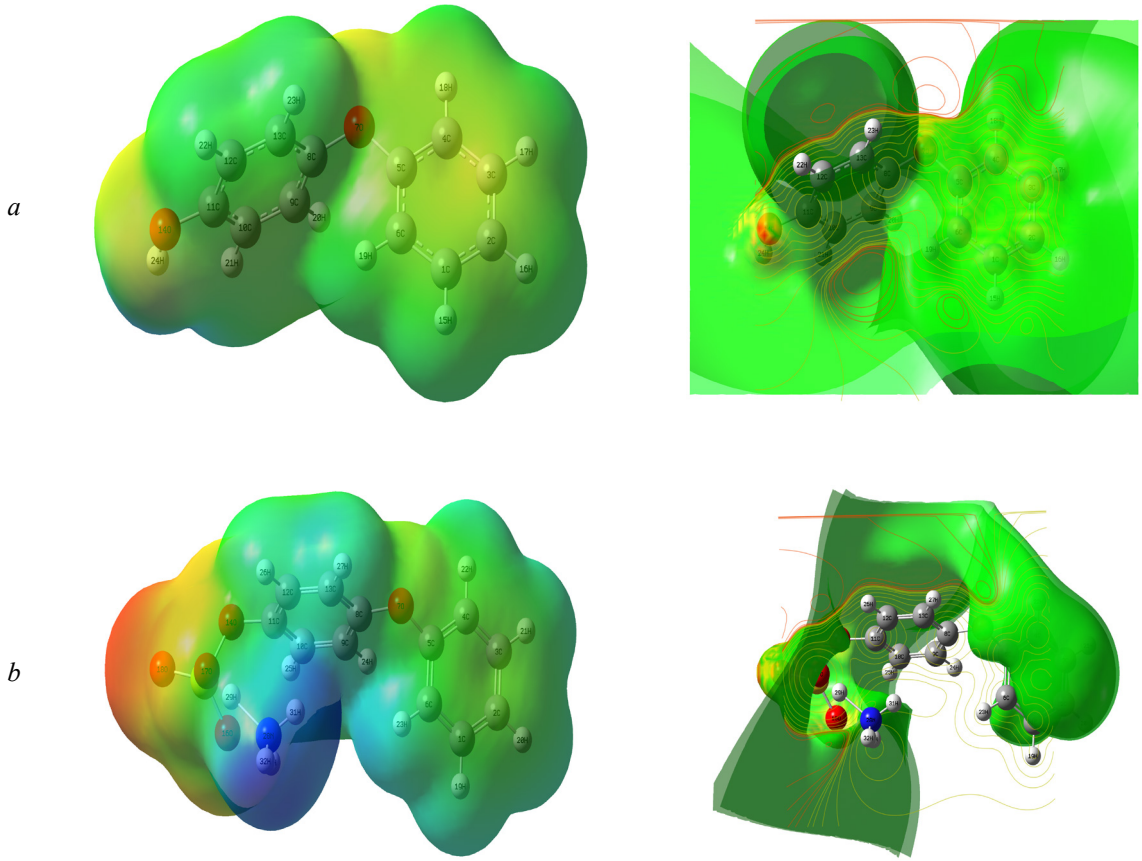


Fig. 3. MEP (left) and and ESP (right) surfaces of *a*) 405 and *b*) 405 sulf, calculated at the B3LYP/6-31G(d,p) level of theory

Table 4. The selected important vibrational frequencies ($cm^{-1}$) determined theoretically (scaled by a factor of 0.9608) and experimentally for 4-O-5 lignin dimer (a) and 4-O-5 sulfated lignin dimer (b)

| a | | | b | | |
|---|---|---|---|---|---|
| Assignments | Theo. | Exp. [25] | Assignments | Theo. | Exp. [25] |
| υO-H | 3675 | 3400–3600 | υN-H | 3476–3337, 2158, 1620, 1603, 1478 | 3400–3600 |
| υC-H | 3095–3044 | 2950–2900 | υC-H | 3105–3060 | 2950–2900 |
| υC=C | 1607–1268 | 1600–1500 | υC=C | 1597–1277 | 1600–1500 |
| υC-O | 1262, 1224, 1179 | 1150–1220 | υC-O | 1240, 1183, 1169 | 1150–1220 |
| | | | υS-O | 1310, 1102, 861, 655 | 1250–1245 |

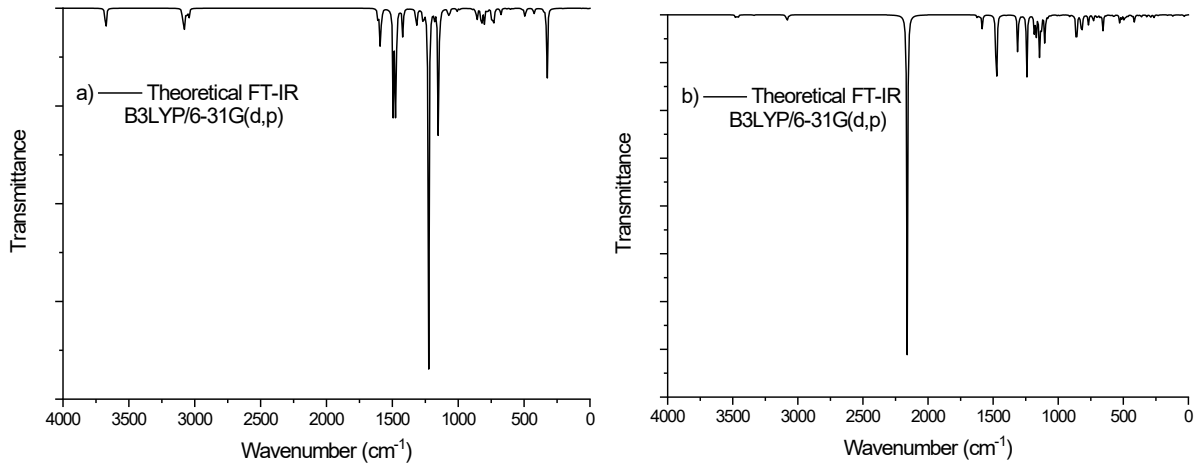



Fig. 4. Calculated FT-IR spectra of a) 4-O-5 lignin dimer and b) 4-O-5 sulfated lignin dimer, calculated at the B3LYP/6-31G(d,p) level of theory

### *Conclusions*

In this work, a systematic study of the effect of sulfation on the structural, electronic and vibrational properties of the model 4-O-5 lignin dimer was carried out using the density functional theory (DFT) method at the B3LYP/6-31G(d,p) level. A comparative analysis of the optimized geometries showed that the introduction of a sulfate group leads to significant changes in the key parameters of the molecule: an increase in the C5-O7 bond length (from 1.3797 to 1.3864 Å) and a decrease in the O7-C8 bond length (from 1.3878 to 1.3770 Å), as well as to a redistribution of valence angles, especially in the region of the ether bridge and the sulfur atom, which indicates a rearrangement of the electron density as a result of the modification.

Mulliken and APT charge analysis revealed a strong positive polarization of the sulfur atom (charge +1.3287 according to Mulliken, +2.4473 according to APT), which is typical for six-digit sulfur in sulfate groups, and a significant increase in the negative charge on the oxygen atoms of the sulfate fragment, especially on O17 (-0.60104 and -1.00392, respectively). This confirms the pronounced electron-withdrawing character of the sulfate group and its influence on the electronic structure of the molecule.

Calculation of the frontier molecular orbitals showed an increase in the HOMO–LUMO energy gap from 5.408 eV to 5.570 eV after sulfation, indicating an increase in the kinetic stability of the molecule. However, the simultaneous increase in electronegativity ($\chi$) from 3.0394 to 3.4772 eV and electrophilicity index ($\omega$) from 1.7081 to 2.1706 eV indicates an increased tendency of the sulfated form to electrophilic reactions, despite its greater stability. A decrease in the nucleophilicity index (N) from 0.5854 to 0.4607 also confirms a change in the reaction profile of the molecule.

Analysis of the molecular electrostatic potential (MEP) surface demonstrated a significant increase in the negative potential in the region of the sulfate group, which explains the improved polarity, the ability to form hydrogen bonds and, as a result, an increase in hydrophilicity and solubility of the modified lignin in aqueous media.

Theoretical IR spectra confirmed the successful modeling of the sulfate derivative: characteristic S-O stretching bands are observed at 1310, 1102, 861 and 655 $cm^{-1}$. These bands can serve as markers for identifying sulfate groups in experimental studies.

The results obtained collectively show that sulfation has a profound effect on the electronic and steric organization of the 4-O-5 structural fragment of lignin, changing its reactivity, stability, and intermolecular interactions. These data contribute to a deeper understanding of the mechanisms of chemical modification of lignin and can be used to develop new strategies for its functionalization for applications in biopolymers, dispersants, drug systems, and other areas of green chemistry.

**Acknowledgments**
*The authors thank the University of Bingöl for the server and the University of Bitlis Eren for the Gaussian 09W software.*

**Funding**
*This work was supported by budget project no. FWES-2026-0011 for the Institute of Chemistry and Chemical Technology, the Siberian Branch of the Russian Academy of Sciences.*

**Conflict of Interest**
*The authors of this work declare that they have no conflicts of interest.*

**Open Access**
*This article is distributed under the terms of the Creative Commons Attribution 4.0 International License (https://creativecommons.org/licenses/by/4.0/), which permits unrestricted use, distribution, and distribution in any medium provided you give appropriate credit to the original author(s) and the source and link to the Creative Commons license, and indicate if they were modified.*

## *References*

1. Boerjan W., Ralph J., Baucher M. *Annu. Rev. Plant Biol*., 2003, vol. 54, pp. 519–546.
2. Vanholme R., Morreel K., Ralph J., Boerjan W. *Curr. Opin. Plant Biol*., 2008, vol. 11(3), pp. 278–285. https://doi.org/10.1016/j.pbi.2008.03.005.
3. Gosselink R.J.A. *Lignin as a renewable aromatic resource for the chemical industry*. Wageningen University, 2011, 191 p.
4. Nguyen L.T., Phan D.-P., Sarwar A., Tran M.H., Lee O.K., Lee E.Y. *Ind. Crops Prod*., 2021, vol. 161, 113219. https://doi.org/10.1016/j.indcrop.2020.113219.
5. Lora J.H., Glasser W.G. *J. Polym. Environ*., 2002, vol. 10(1-2), pp. 39–48.
6. Jeevanantham V., Jagatheesan R., Vinitha M., Snega P. *Handbook of Lignin*. Springer, Singapore, 2025, pp. 1–22. https://doi.org/10.1007/978-981-97-2664-6_27-1.
7. Kuznetsov B.N., Vasilyeva N.Y., Kazachenko A.S., Levdansky V.A., Kondrasenko A.A., Malyar Yu.N., Skvortsova G.P., Lutoshkin M.A. *Wood Sci. Technol*., 2020, vol. 54, pp. 365–381. https://doi.org/10.1007/s00226-020-01157-6.
8. Nadányi R., Ház A., Lisý A., Jablonský M., Šurina I., Majová V., Baco A. *Energies*, 2022, vol. 15, 6520. https://doi.org/10.3390/en15186520.
9. Rahmani A., Abdulkhani A., Ashori A., Hosseinzadeh J. *Sci. Rep*., 2024, vol. 14, 28932. https://doi.org/10.1038/s41598-024-80256-x.
10. Kazachenko A.S., Akman F., Holikulov U., Jumabaev A., Malyar Yu.N. *Mendeleev Commun*., 2026, vol. 36, 260. https://doi.org/10.71267/mencom.7910.
11. Onley J.R., Gupta K., de Raad M., Bowen B.P., Tan S., Yoder S., Sale K.L., Singh A.K., Simmons B.A., Adams P.D., Northen T.R., Deng K. *Sci. Rep*., 2025, vol. 15, 10296. https://doi.org/10.1038/s41598-025-88571-7.
12. Xiao L.-P., Lv Y.-H., Yang Y.-Q., Zou S.-L., Shi Z.-J., Sun R.-C. *Int. J. Mol. Sci*., 2023, vol. 24, 10304. https://doi.org/10.3390/ijms241210304.
13. Richel A., Vanderghem C., Simon M., Wathelet B., Paquot M. *Anal. Chem. Insights*, 2012, vol. 7, pp. 79–89. https://doi.org/10.4137/ACI.S10799.
14. Karmanov A.P., Ermakova A.V., Raskosha O.V., Bashlykova L.A., Rachkova N.G., Kocheva L.S. *Khimiya Rastitel'nogo Syr'ya*, 2023, no. 4, pp. 5–28. https://doi.org/10.14258/jcprm.20230412560. (in Russ.).
15. Luo Z., Qian Q., Sun H., Wei Q., Zhou J., Wang K. *Energies*, 2023, vol. 16, 125. https://doi.org/10.3390/en16010125.
16. Becke A.D. *J. Chem. Phys*., 1993, vol. 98(7). https://doi.org/10.1063/1.464913.
17. Lee C., Yang W., Parr R.G. *Phys. Rev. B*, 1998, vol. 37(2). https://doi.org/10.1103/PhysRevB.37.785.
18. Frisch M.J., Trucks G.W., Schlegel H.B. et al. *Gaussian 09, Revision D.1*. Gaussian, Inc., Wallingford CT, 2009.
19. Dennington R., Keith T., Millam J. *GaussView, Version 6*. Semichem Inc., Shawnee Mission, KS, 2016.
20. Khudaykulov B., Norkulov A., Holikulov U., Absanov A., Doroshenko I., Jumabaev A. *J. Low Temp. Phys*., 2025, vol. 51(2). https://doi.org/10.1063/10.0035406.
21. Akman F., Kazachenko A.S., Malyar Y. *Cellulose Chem. Technol*., 2021, vol. 55(1-2), pp. 41–54. https://doi.org/10.35812/CelluloseChemTechnol.2021.55.05.
22. Becke A.D. *J. Chem. Phys*., 1993, vol. 98(7), pp. 5648–5652.
23. Jabha M., El Alaoui A., Jarid A., Houssine Mabrouk E. *Optical Fiber and Applications*. IntechOpen, 2023. http://dx.doi.org/10.5772/intechopen.109250.
24. Krivdin L.B. *Molecules*, 2021, vol. 26, 2450. https://doi.org/10.3390/molecules26092450.
25. Kazachenko A.S., Akman F., Vasilieva N.Y., Malyar Y.N., Fetisova O.Y., Lutoshkin M.A., Berezhnaya Y.D., Miroshnikova A.V., Issaoui N., Xiang Z. *Polymers*, 2022, vol. 14, 3000. https://doi.org/10.3390/polym14153000.
26. Makaveckas T., Šimonėlienė A., Šipailaitė-Ramoškienė V. *Sustainability*, 2025, vol. 17(21), 9913. https://doi.org/10.3390/su17219913.
27. Carbó-Dorca R., Bultinck P. *J. Math. Chem*., 2004, vol. 36, pp. 231–239. https://doi.org/10.1023/B:JOMC.0000044221.23647.20.
28. Masnabadi N., Thalji M.R., Alhasan H.S., Mahmoodi Z., Soldatov A.V., Ali G.A.M. *Molecules*, 2022, vol. 27, 4011. https://doi.org/10.3390/molecules27134011.

29. Jumabaev A., Khudaykulov B., Holikulov U., Norkulov A., Subbiah J., Al-Dossary O.M., Hushvaktov H., Absanov A., Issaoui N. *Opt. Mater*., 2025, vol. 159, 116683. https://doi.org/10.1016/j.optmat.2025.116683.
30. Chen D., Wang H. *Proc. Combust. Inst*., 2019, vol. 37(1), pp. 953–959. https://doi.org/10.1016/j.proci.2018.06.120.
31. Elshakre M.E., Noamaan M.A., Moustafa H., Butt H. *Int. J. Mol. Sci*., 2020, vol. 21, 1253. https://doi.org/10.3390/ijms21041253.
32. Sharma D., Tiwari S.N. *J. Mol. Liq*., 2016, vol. 214, pp. 128–135. https://doi.org/10.1016/j.molliq.2015.11.045.
33. Zheng Q., Nong G., Li N. *Polymers*, 2024, vol. 16, pp. 1237. https://doi.org/10.3390/polym16091237.

*Received April 6, 2026.*

*Revised April 17, 2026*

*Accepted April 24, 2026*

**Information about authors**

*Kazachenko Alexander Sergeyevich* – PhD, Associate Professor, leo_lion_leo@mail.ru
*Akman Feride* – PhD, Professor, chemakman@gmail.com
*Holikulov Utkirjon* – DSc, Department of Optics and Spectroscopy, utkirxolikulov12@gmail.com
*Jumabaev Abduvakhid* – DSc, Department of Optics and Spectroscopy, jumabaev2@rambler.ru
*Malyar Yuriy Nikolaevich* – PhD, yumalyar@gmail.com